Performance Enhancement for Visible Light Communication Based ADO-OFDM

Samir M. Hameed (samirmhameed@uoitc.edu.iq)
University of Information Technology and Communications.UOITC https://orcid.org/0000-0003-0179-1409

Sinan M. Abdulsatar
University of Technology/Electrical Engineering Department

Atheer A. Sabri
University of Technology/Communication Engineering Department

Research Article

Keywords: ADO-OFDM, Visible light communication (VLC), DCO-OFDM, ACO-OFDM, Hamming coding.

Posted Date: March 30th, 2021

DOI: https://doi.org/10.21203/rs.3.rs-307923/v1

Performance Enhancement for Visible Light Communication Based ADO-OFDM

Samir M. Hameed[1], Sinan M. Abdulsatar [2], Atheer A. Sabri[3]

[1] *University of Information Technology and Communications, Baghdad, Iraq*
[2]*Electrical Department, University of Technology, Baghdad, Iraq*
[3]*Communication Department, University of Technology, Baghdad, Iraq*
[*]Corresponding author: samirmhameed@uoitc.edu.iq

Abstract

The increasing demand for bandwidth through modern applications and multimedia services has led to high-speed wireless communications. Optical Wireless Communications (OWC) encourages solutions that provide a higher data rate due to the large bandwidth available. In this paper, performance enhancement approaches will be studied and simulated for Visible Light Communication (VLC) as a case study. The Orthogonal Frequency Division Multiplexing (OFDM) systems are used to investigate Intensity Modulation/ Direct Detection (IM/DD) to improve the performance of VLC. The IM/DD in OWC requires positive real OFDM symbols, so there are many approaches to satisfy this requirement. This paper proposed a model of Asymmetrically Clipped DC-Biased Optical (ADO-OFDM) to use in OWC/VLC environment. The Proposed system has avoided the use of the noise cancelation technique that is used in traditional ADO-OFDM. The results show that the ADO-OFDM has the best spectral efficiency than DC-biased Optical (DCO-OFDM) and Asymmetrically Clipped Optical (ACO-OFDM). Also, it has better optical efficiency than DCO-OFDM with the equally overall Bit Error Rate (BER) at the same signal-to-noise ratio. Hamming channel coding/decoding with different code lengths is applied in various optical OFDM schemes for BER improvements. Furthermore, we simulate and analyze these optical OFDM systems with many modulation orders.

Keywords: ADO-OFDM, Visible light communication (VLC), DCO-OFDM, ACO-OFDM, Hamming coding.

1-Introduction

Wireless communication can be categorized into two different types, Radio Frequency (RF) and Optical Wireless Communication (OWC). Higher data rates increasing demands are growing as users requirement causes congestion in the RF existing spectrum [1]. Today, the Internet of Things (IoT) networks have gained almost importance due to connecting and exchanging data between an enormous number of embedded sensors and devices over the internet. The OWC can take an essential rule for satisfying the IoT requirement for high data rate and a real-time communication system for future communication networks, including Fifth- and Sixth-Generation (5G and 6G, respectively) communication systems [2]–[4]. The OWC based Visible Light Communication (VLC) has been of tremendous interest for indoor communication due to high data rate, low cost, and security [5]–[7]. The VLC uses the Light Emitting Diode (LED) as a light source, satisfying both communication and illuminations simultaneously [5]. Orthogonal Frequency Division Multiplexing (OFDM) has been commonly used in VLC systems in recent years [8]–[10], due to its high spectral efficiency and the Intersymbol Interference (ISI) resistance. The OFDM symbols can be represented as intensity for optical wireless communication, which means the modulated signals are both real and positive; however, the baseband OFDM signals usually are complex and bipolar [11]. The Intensity Modulation with Direct Detection (IM/DD) is easy and straightforward to apply with OFDM. Hermitian symmetry conversion is appropriate for the Inverse Fast Fourier Transform (IFFT) for producing real signals [12]. In IM/DD, different unipolar OFDM methods can be used, such as DC-Offset (DCO-OFDM) [13], Asymmetrically Clipped Optical (ACO-OFDM), and Asymmetrically Clipped DC Biased Optical (ADO-OFDM), which is a hybrid of both ACO-OFDM and DCO-OFDM [14], [15]. In this paper, an enhancement model for ADO-OFDM is proposed first, which reduces the complexity of the traditional ADO-OFDM receiver. Then DCO-OFDM, ACO-OFDM, and the proposed model of ADO-OFDM systems are tested in the VLC environment, a comparison between these systems is achieved. Hamming channel coding/decoding is used with the proposed model and other optical OFDM schemes. Simulation results show the enhanced ADO-OFDM gives the best performance in the OWC / VLC environment. The rest of the paper is organized as section 2 system model, section 3 proposed enhancement model, section 4 simulation results, and section 5 conclusions.

2. System Model

The performance of OWC depends on the type of system used, the transmitter used, the laser or LED, and propagation via channel Line of Sight (LOS) or diffused. We can reach high data rates in VLC based LOS, but the receiver is susceptible to shadowing effect, and it must be aligned with the transmitter. In diffuse VLC, there are many light paths in a system from source to receiver, making the system resilient to block/shadow [16]. Optical OFDM increases optical power efficiency and decreases the ISI with minimum acceptable bit error rate (BER) compared to typical optical modulation systems [16]–[18]. This section describes the features of different optical OFDM such as DCO-OFDM, ACO-OFDM, and ADO-OFDM. Furthermore, the indoor VLC model features and characteristics are presented.

2.1. Optical OFDM

At the optical OFDM transmitter, digital signals are modulated using either different orders of M-ary Quadrature Amplitude Modulation(MQAM) or M-ary Phase Shift Keying (MPSK) and mapped to symbols with complex values represented by [X_1, X_2,…X_N]. The data is converted from serial to parallel at OFDM framing and Hermitian symmetry block, as shown in Fig. 1. The input symbols to the IFFT block after applying as Hermitian symmetry can be written as [11], [14]:

$$X_{N-m} = X_m^{*} \quad m = 0,1, \ldots \frac{N}{2} \tag{1}$$

$$X_0 = X_{N/2} = 0 \tag{2}$$

Where X_m^{*} is complex conjugate, by taking IFFT into OFDM symbols and applying (1) and (2), the output time domain is determined as [19], [20]:

$$X_n = \frac{1}{N}\sum_{m=0}^{N-1} X_m e^{\frac{i2\pi nm}{N}} \quad \text{for } 0 \le n \le N\text{-}1 \tag{3}$$

Where N is the number of IFFT points, the OFDM symbols (X_n) are real vales after Hermitian symmetry, but the signals are bipolar. Only positive signals with real values can transmit in IM/DD or OWC systems [14], [15]. There are two methods for converting bipolar signals to unipolar, DC-biased in DCO-OFDM and zero clipping in ACO-OFDM [11].

The Cyclic Prefix (CP) is very important to prevent the ISI; the CP is appended at the beginning of each OFDM frame as a guard interval. The output sequence can be described by adding CP as a copy of the OFDM symbol's last portion [11]:

$$X_{CP} = [X_{N-G} \ \ldots X_{N-1}, X_0 \ldots X_{N-1}] \quad (4)$$

Where G is the CP length and is chosen longer than the delay spread of the channel [13]. The sequence at (4) is converted to a continuous signal by a Digital to Analog Converter (DAC). The OFDM signal becomes ready for transmission by LED, which satisfies IM/DD requirements. The optical intensity signal is transmitted through the OWC channel, and the photodetector detected the optical signal. It converted it into an electrical signal on the receiver side, as shown in Fig. 1. The non-distorted received signal with existing Additive white Gaussian noise (AWGN) is given as [11]:

$$y(t) = x(t) + w(t) \quad (5)$$

Where w(t) is AWGN, and x(t) is the transmitted signal. The electrical signal is prepared for OFDM demodulation processing using the Analog-to-Digital conversion (ADC) and serial-to-parallel conversion. The CP is removed, and a Fast Fourier Transform (FFT) is applied to extract the original modulated symbols [16], [19].

The FFT of N point is applied to (5) to obtain [11], [13]:

$$Y_m = \sum_{n=0}^{N-1} X_n e^{\frac{-i2\pi nm}{N}} + W_m \quad \text{for } 0 \leq \text{m} \leq \text{N-1} \quad (6)$$

Where W is the noise component at the receiver after FFT operation and is written as [11], [13]:

$$W_m = \sum_{n=0}^{N-1} w_n e^{\frac{-i2\pi nm}{N}} \quad \text{for } 0 \leq \text{m} \leq \text{N-1} \quad (7)$$

The output from (6) is de-framing by converting complex symbols from parallel to serial and extract the information by demodulating process.

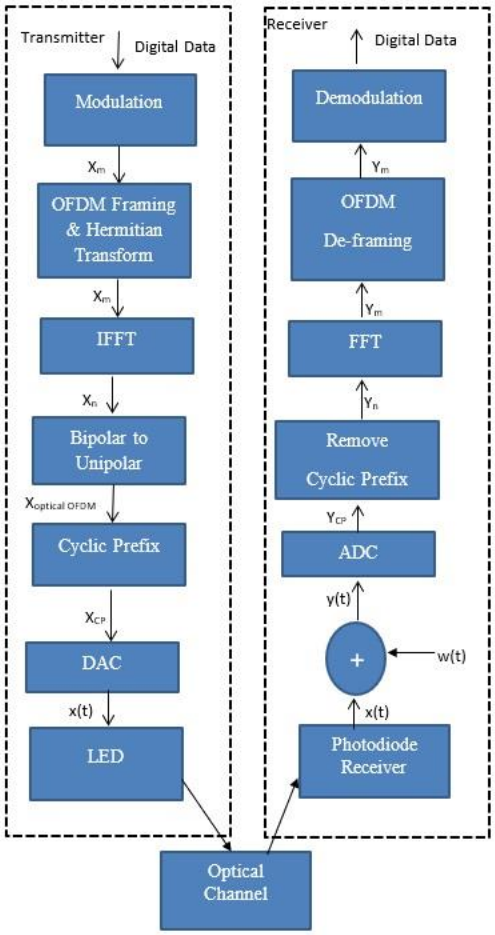

Fig. 1 General Optical OFDM System

2.2 VLC Model

It is necessary to study the received power and the path loss in typical environments due to the indoor OWC/VLC channel [13]. There are two link types inside the room: dominant direct link LOS and non-dominant diffuse links arise due to light reflection through the walls, floor, and ceiling [21]. The received power at any point (x,y,z) inside the room and neglecting the diffuse links is given by [13]:

$$P_r = H(0)P_t \tag{8}$$

Where P_t is the transmitted power by LEDs for the transmitted OFDM signal, and H(0) is the DC gain of the indoor OWC/VLC channel impulse response. The Lambertian distribution represents the radiated intensity by [7], [22]:

$$R(\Phi) = \frac{(ml+1)}{2\pi}\ cos^{ml}(\Phi) \quad for -\frac{\pi}{2} \leq \Phi \leq \frac{\pi}{2} \tag{9}$$

Where Φ is the irradiance angle, and ml is the Lambertian index is given as:

$$\text{ml} = \frac{-\ln(2)}{\ln(\cos \Phi_{\frac{1}{2}})} \tag{10}$$

Where $\Phi_{½}$ is half illumination angle and also is called (Radiation semi- angle) [21]

Thus, the LOS channel impulse response for indoor OWC/VLC is modeled as [22][21]:

$$H(t) = \frac{A(ml+1)}{2\pi d^2}\ cos^{ml}(\Phi) T(\Psi) g(\Psi)\ cos(\Psi) \tag{11}$$

Where d is the distance between the transmitter and the receiver, and A is the photodetector physical area. The photodetector is collecting the light at an incidence angle Ψ, and Ψ_c is the Field of View (FOV) angle for the receiver, which is $\Psi_c \leq \Phi_{½}$ [15]. $T(\Psi)$ is the transmission filter, and $g(\Psi)$ is the receiver concentrator filter that is characterize by lens refractive index of photodetector (n_{len}) as follow [19]:

$$g(\Psi) = \frac{{n_{len}}^2}{sin\,{\Psi_c}^2} \qquad for\ 0 \leq \Psi \leq \Psi_c \tag{12}$$

Substituting (11) in (8), and let $T(\Psi)$ the transmission filter gain is unity, the power at the detector is written as :

$$P_r = P_t .\ \frac{A(ml+1)}{2\pi d^2}\ cos^{ml}(\Phi)\ cos(\Psi) g(\Psi) \tag{13}$$

Thus, from (5) and using (11), the received signal by photodetector can be re-written as [19] :

$$y(t) = h(t) * x(t) + w(t) \tag{14}$$

Where x(t) is the emitted signal by LEDs, and w(t) is the AWGN that is added in the electrical domain.

2.3 DCO-OFDM

At the DCO-OFDM transmitter, the modulated complex symbols [X_1, X_2,… X_N] are assigned to the IFFT after applying Hermitian symmetry. The number of subcarriers available for data is (N/2-1), so the spectral efficiency is reduced by about 50% from traditional OFDM due to Hermitian symmetry [12]. The DC bias is used in DCO-OFDM to convert the bipolar signal to unipolar, as shown in Fig. 2. The added DC bias is responsible for shifting the OFDM symbols before clipping. The output DCO-OFDM is written by change (3), and it becomes [8]:

$$X_{DCO} = \frac{1}{N}\sum_{m=0}^{N-1} X_m e^{\frac{i2\pi nm}{N}} + \beta dc \quad \text{for } 0 \le m \le N\text{-}1 \qquad (15)$$

Where βdc is DC bias could be added and selected concerning the standard deviation of the DCO-OFDM signal [6]. The performance of DCO-OFDM is strongly affected by the DC bias, as the optical power efficiency of the system decreases [8], [12], [14].

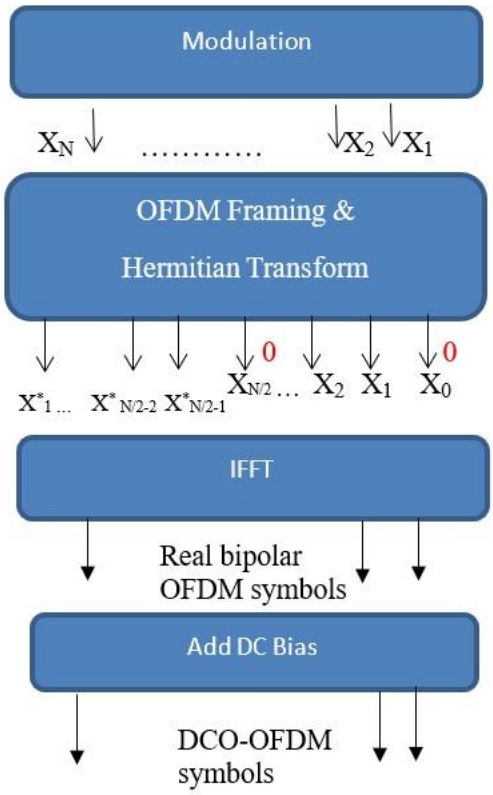

Fig. 2 DCO-OFDM Generation System

2.4 ACO-OFDM

In ACO-OFDM, data symbols are transmitted by the only odd subcarriers, and the modulated symbols are distributed over (N/4) subcarriers. The spectral efficiency of ACO-OFDM is reduced by 25% of traditional OFDM and 50% of DCO-OFDM spectral efficiency [14]. The input symbols to IFFT are mapped across only odd subcarriers and the even subcarriers represented by zero as:

$$[0, X_1, 0, X_3, \ldots X_{N/2-1}] \quad (16)$$

The output of IFFT becomes real after applying Hermitian symmetry in (1) and (2). The clipping at zero technique is used at bipolar to unipolar block in Fig. 3. As in (15), The ACO-OFDM output can be written as:

$$X_{ACO} = \begin{cases} X_n & if\ X_n \geq 0 \\ 0 & if\ X_n < 0 \end{cases} \quad (17)$$

Where X_n is obtained from (3), due to the anti-symmetry property, there is no data loss in the clipping process [18]. The Optical power efficiency of ACO-OFDM is better than DCO-OFDM because it doesn't need DC bias [15]. To compensate for the bitrate loss gap, we can increase the modulation order of MQAM or MPSK, which means an increase in the number of bits ($\log_2 M$) per OFDM symbol [9].

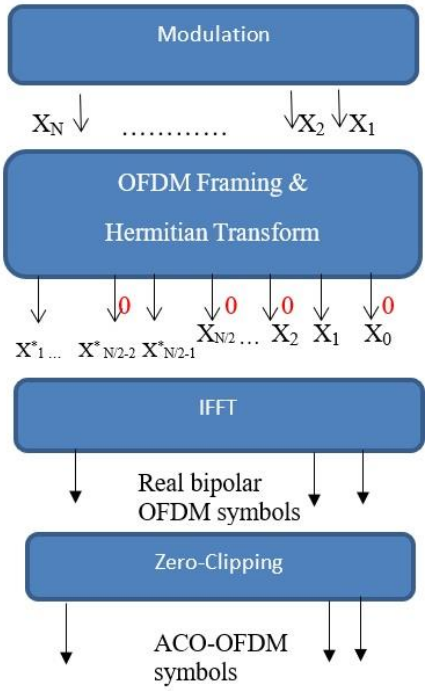

Fig. 3 ACO-OFDM Generation System

2.5 ADO-OFDM

ADO-OFDM is a technology that imposes the performance of spectral efficiency; it is a combination of both DCO-OFDM and ACO-OFDM [12], [14], [17], [19]. The odd subcarriers are transmitted using ACO-OFDM, where DCO-OFDM sends even subcarriers [14]. The generated ADO-OFDM is given by [19]:

$$X_{ADO} = X_{ACO} + X_{DCO} \tag{18}$$

On the receiver side, the odd subcarriers are demodulated as ACO-OFDM, wherein even subcarriers are demodulated after the noise cancellation process [12], [14], [17], [19]. The optical power efficiency of ADO-OFDM is better than ACO-OFDM because it relies on DC bias only for even subcarriers [14][10].

3. Proposed Enhancement Model

Many others suggested several techniques to enhance the spectral efficiency based on optical OFDM [8], [15], [23], [24]. This section describes the proposed model of ADO-OFDM features and the details for the system design. The proposed system reduces the complexity of the traditional ADO-OFDM receiver. We introduce a scheme by transmitting constellation sizes unequally with even and odd subcarriers in the proposed approach to increase the data rates. Furthermore, the Hamming channel coding is utilizing in BER enhancement for our proposed system and OFDM optical systems.

3.1 The Proposed Model of ADO-OFDM System

The proposed ADO-OFDM transmitter consists of a Hamming channel encoder and MQAM modulator. The encoded/modulated symbols X are divided into odd and even variables, X_{odd} and $X_{even,}$ respectively. The odd subcarriers in ADO-OFDM are transmitted using ACO-OFDM, where even subcarriers are sending via DCO-OFDM, as shown in Fig. 4. The Hermitian symmetry applies for both ACO-OFDM and DCO-OFDM components [17], [19], where:

$$X_{odd} = [0, X_1, 0, X_3, 0, \dots \dots, X_{N-1}\ ] \tag{19}$$

$$X_{even} = [\ X_0, 0, X_2, 0, \dots, X_{N-2}, 0\ ] \tag{20}$$

The ACO-OFDM symbols in the time-domain are generated after the IFFT process to X_{odd}. The output symbols have real values due to Hermitian symmetry but bipolar.

They are converted to unipolar by clipping the negative values by setting them to zero. Also, the DCO-OFDM signals are created after IFFT and are converted to unipolar by adding β_{dc} to get non-negative output. We propose a variable DC bias by taking the minimum value of each OFDM symbol, then taking the absolute value, and adding it to the signal to get a non-negative output. The resulting ADO-OFDM signal is (X_{ACO} +X_{DCO}), then adding CP and converted to analog by (DAC) and transformed to LED's intensity light.

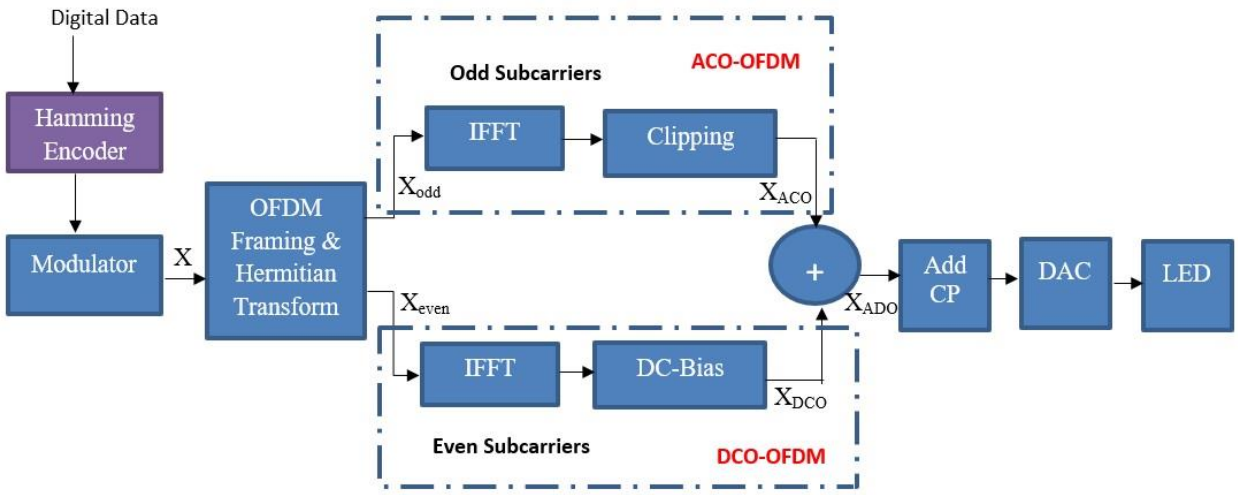

Fig. 4 The Proposed ADO-OFDM Transmitter System

On the receiver side, firstly, the optical signal transformed to an electrical signal by the photodetector, converted to digital, removing CP, and then passes to IFFT, as shown in Fig. 5. Our proposed ADO-OFDM receiver has two paths, the direct path that we call ACO-OFDM demodulation and the other called DCO-OFDM reconstruction. The ACO-OFDM symbols in the odd subcarriers are straightly recovered and demodulated in a direct path. The demodulated bits are then re-modulated again using ACO-OFDM to recover the DCO-OFDM symbols and subtract from the overall received signal. Now, The information on the even subcarriers is ready for the demodulation process. Then the odd and even data are rearranged, and the original data extracted after the demodulation and decoding process. The proposed receiver reduces the design complexity by overcoming the uses of the ACO-OFDM noise estimation block as mentioned in references [12], [14], [19]. Also, the noise estimation can work only in a flat channel [14]. We can

use (N/2-1) of subcarriers in ADO-OFDM for data transmission as in DCO-OFDM. We can increase our proposed system's spectral efficiency and data rate higher than DCO-OFDM by using different modulation consultation sizes for odd and even subcarriers, respectively, M_{ACO} and M_{DCO}. Consider the following example for spectral efficiency comparison as in Table 1 by assuming N=64.

Table 1 Example for Spectral Efficiency Comparison

Optical OFDM	Spectral Efficiency Formulas [10]	Spectral Efficiency (bit/s/Hz)
ACO-OFDM (M_{ACO} =4)	$\frac{\log_2 MACO}{4}$	0.5
DCO-OFDM (M_{DCO} =4),	$\frac{(N-2)\log_2 MACO}{2N}$	0.968
ADO-OFDM (M_{ACO}, M_{DCO} =4)	$\frac{(\log_2 MDCO + \log_2 MACO)}{4} - \frac{\log_2 MDCO}{N}$	0.968
ADO-OFDM (M_{ACO} = 8, M_{DCO} =4)	$\frac{(\log_2 MDCO + \log_2 MACO)}{4} - \frac{\log_2 MDCO}{N}$	1.219

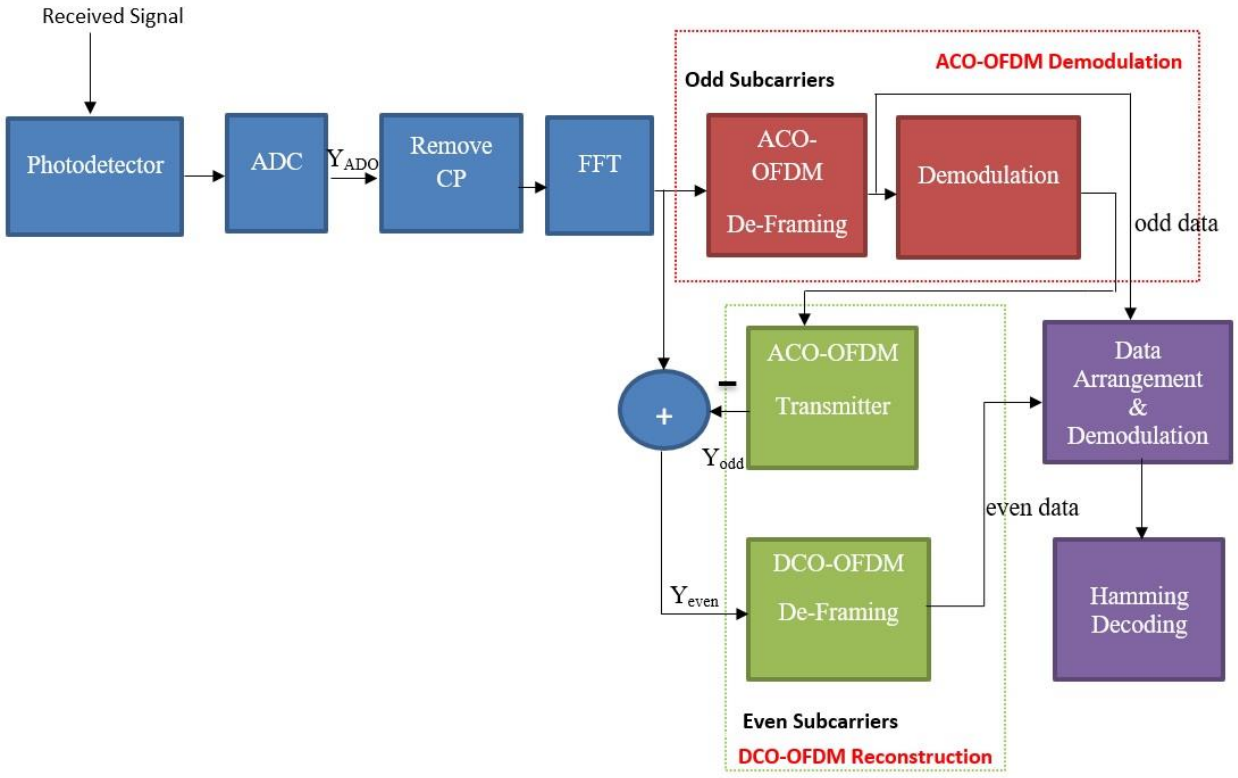

Fig. 5 The Enhanced ADO-OFDM Receiver System

3.2 Hamming Channel Coding/Decoding

Channel coding techniques can be used with optical OFDM to improve system performance by reducing noise effects resulting through transmission, detection, or channel nonlinearity [15], [25]. In [26], channel coding was used to reduce the influence of high-peak to average power in an OFDM system. We can use channel coding with error corrections before the data modulation to compensate for the BER during the data transmission, especially when higher modulation constellation order is used [27]. In this paper, we use Hamming code as one type of linear channel coding in forwarding error correction, and it can be applied with DCO-OFDM, ACO-OFDM, and DCO-OFDM. Hamming code is the right choice for a single error bit correction with simple parity codes[15]. The Hamming codes notation can be written as [26]:

$$(2^r - 1, 2^r - r - 1)_2 \tag{21}$$

Where r number of parity digits and $r \geq 2$, $2^r - 1$ is the length of the Hamming code and $2^r - r - 1$ is the message length. So if r=2, the code is (3,1), and for r= 3, the code (7,4) and so on. The generator matrix G and parity check matrix for (7,4) Hamming code example respectively are:

$$G = \begin{bmatrix} 1 & 0 & 0 & 0 & 1 & 1 & 0 \\ 0 & 1 & 0 & 0 & 1 & 0 & 1 \\ 0 & 0 & 1 & 0 & 0 & 1 & 1 \\ 0 & 0 & 0 & 1 & 1 & 1 & 1 \end{bmatrix} \tag{22}$$

$$H = \begin{bmatrix} 1 & 1 & 0 & 1 & 1 & 0 & 0 \\ 1 & 0 & 1 & 1 & 0 & 1 & 0 \\ 0 & 1 & 1 & 1 & 0 & 0 & 1 \end{bmatrix} \tag{23}$$

4-Simulation Result

In this section, the BER simulations for DCO-OFDM, ACO-OFDM, and the proposed model of ADO OFDM systems are accomplished using a different modulation constellation size of QAM. Matlab software is employed in the simulation, and BER comparison curves are produced using 5000 OFDM symbols, N=1024, and G=N/16, the number of CP is 64. The actual number of subcarriers for data transmission is (256 for ACO-OFDM, 511 subcarriers for both DCO-OFDM and enhanced ADO-OFDM. All these systems are tested with different Signal-to-

Noise Ratios (SNR) in the LOS OWC/VLC channel. Fig. 6 shows a DCO-OFDM BER simulation case for M=2,4,5,7, and 10 with of β_{dc} 0.2V is used in this scheme.

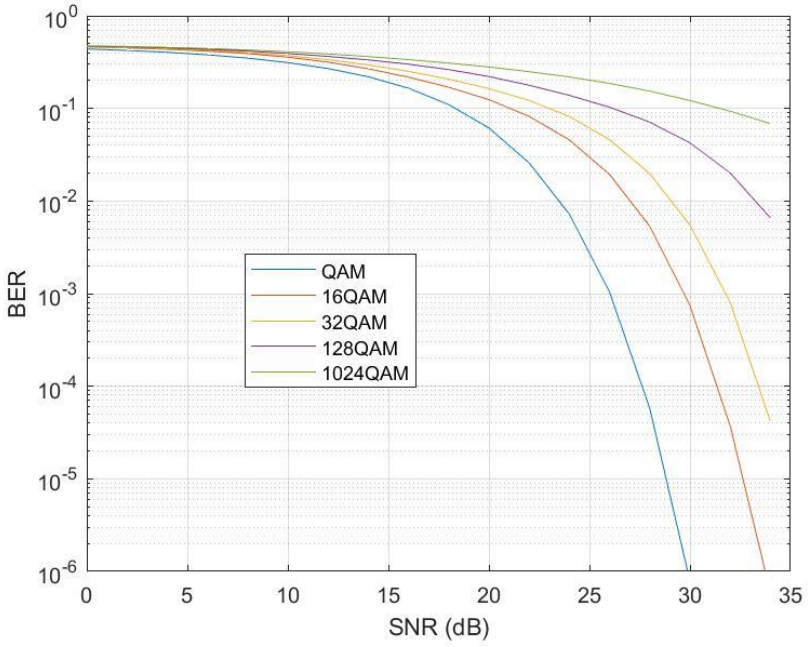

Fig. 6 DCO-OFDM BER Performance.

Figure 7 shows the BER performance of ACO-OFDM, which was tested for M = 2,4,5,7,10, and 12. ACO-OFDM achieves a better BER response than DCO-OFDM, because it does not require bias, while the spectral efficiency is low.

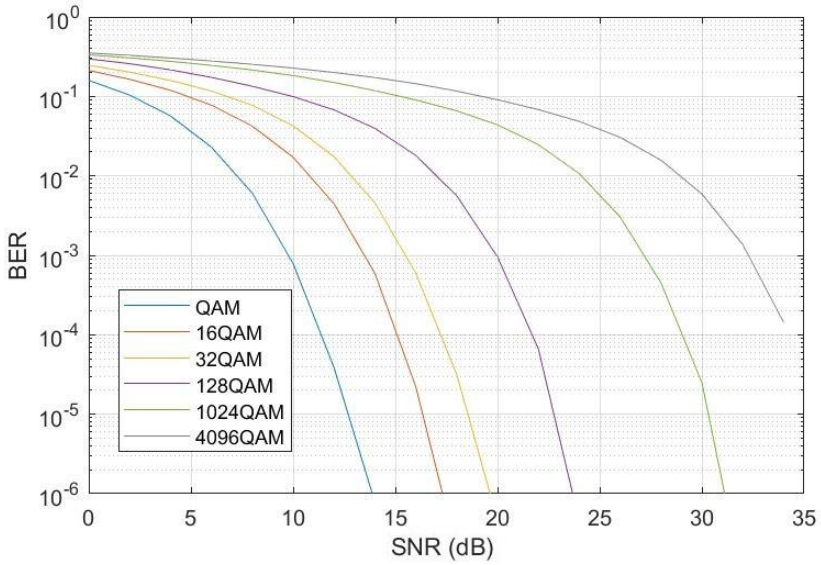

Fig. 7 ACO-OFDM BER Performance.

The proposed model of the ADO-OFDM system mixes both ACO-OFDM for odd subcarriers transmission and DCO-OFDM for even subcarriers. In the simulation, odd subcarriers' size is equal to 256, while even subcarriers are set to 255. Fig. 8 demonstrates the simulation results for the proposed ADO-OFDM performance for different states, equally constellation order for both odd and even subcarriers such as (QAM DCO-OFDM+QAM ACO-OFDM) and unequally M-order such as (QAM DCO-OFDM +16 QAM ACO-OFDM). The β_{dc} values are reduced in the ADO-OFDM and are approximately adaptively in the range $0.09 \leq \beta_{dc} \leq 0.115$. Reduction of β_{dc} due to only 50% subcarriers with DC biasing is used and leads to the enhanced ADO-OFDM system's power utilization.

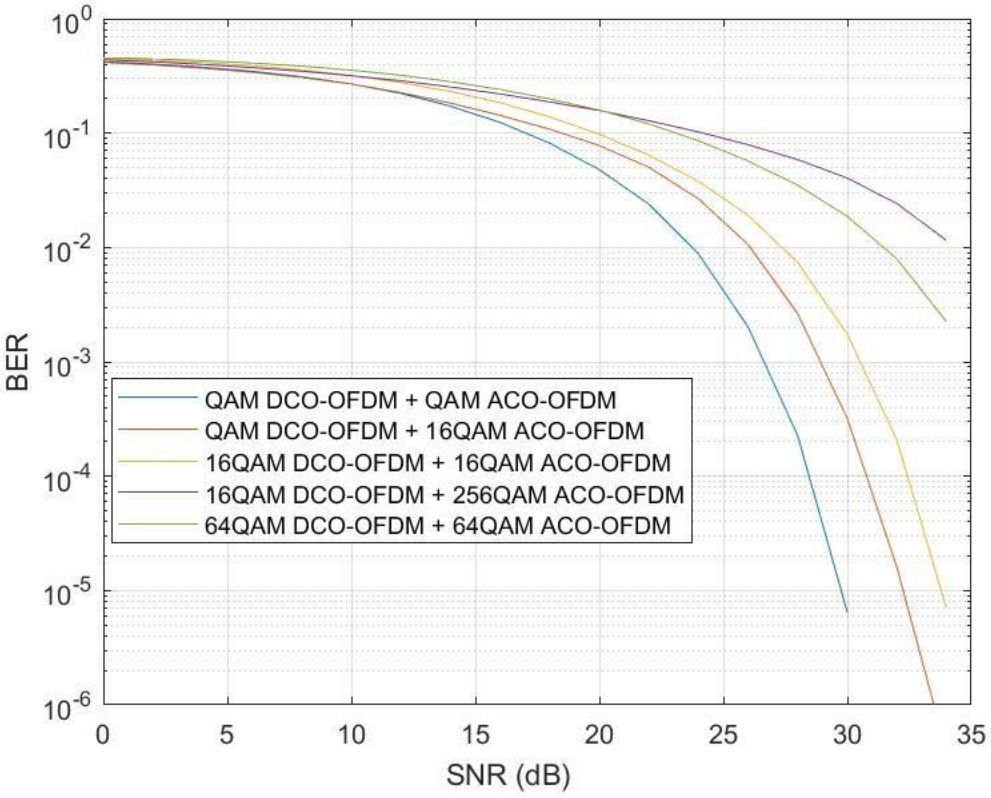

Fig. 8 Proposed Enhanced ADO-OFDM BER Performance.

The simulation results in Figs 6 and 8 show the BER performance similarity for ADO-OFDM and DCO-OFDM. Simultaneously, the ACO-OFDM BER curves are better in Fig. 7 because this scheme uses only half of the sub-carriers compared to the other systems. To make an exact comparison between the different OFDM

optical systems concerning efficient power, we calculate the transmitted optical signal as given in [28]:

$$P_{optical} = E[X_{OFDM}] = \sqrt{\frac{E[X_{OFDM}{}^2]}{\pi}} \quad (24)$$

Where X_{OFDM} is N-point transmitted OFDM (either DCO-OFDM, ACO-OFDM, or ADO-OFDM). Fig. 9 presents a comparison of optical power concerning the number of transmitted subcarriers N. The simulation is carried out for M=4 for both ADO-OFDM and DCO-OFDM, where M=8 is adjusted for ACO-OFDM to investigate the nearest spectral efficiency approximately.

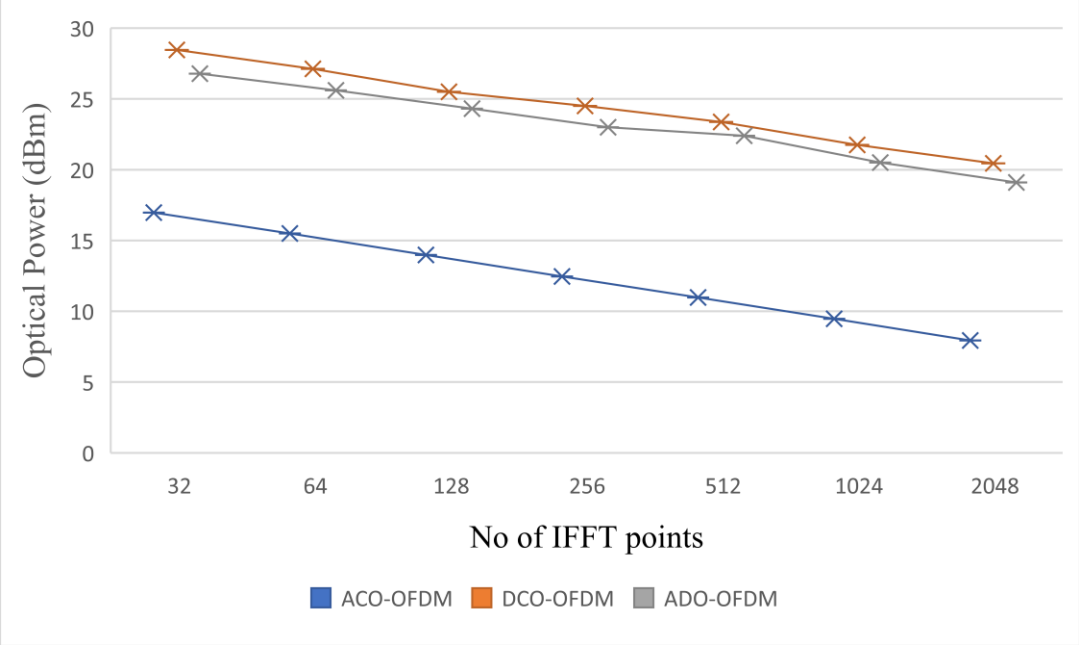

Fig. 9 Optical Transmitted Power for Various Optical OFDM Systems.

We can see from Fig.9 the proposed ADO-OFDM optical power efficiency is better than DCO-OFDM, while the ACO-OFDM is the best response because it does not need DC biasing. Also, we tested the proposed system for unequal constellation size for odd and even subcarriers; it gives better power efficiency than equally constellation size about 1dBm. Hamming coding/decoding is used with our proposed system and other schemes to compensate for the BER performance.

Fig.10 presents Hamming coding/decoding advantages for performance enhancement for different optical OFDM. To achieve a BER comparison, we use various lengths of message and code such as (3,1), (7,4), and (15,11). We can see that the Hamming codes improve performance by correcting the bit errors due to AWGN and channel response. Although (3,1) coding gives the best result, it reduces the spectral efficiency by the rate (1/3), while (7,4) and (15,11) coding scheme reduces the spectral efficiency by (4/7) and (11/15), respectively. Table 2 summarizes the BER comparisons between the systems, using M= 4 for both DCO-OFDM and enhanced ADO-OFDM and M= 8 for ACO-OFDM.

Table 2 BER Performance and Spectral Efficiencies Comparison

Scheme	(SNR) in dB at BER=$1*10^{-4}$	(SNR) in dB at BER=$1*10^{-5}$	Spectrual Efficency (bit/s/Hz)
DCO-OFDM (without coding)	32	33	0.998
Hamming coding (3,1)	27	28	0.331
Hamming coding (7,4)	28	29	0.57
Hamming coding (15,11)	29	30	0.732
ACO-OFDM (without coding)	28.5	31	0.75
Hamming coding (3,1)	18	22	0.25
Hamming coding (7,4)	21.5	22.5	0.429
Hamming coding (15,11)	21.7	22.7	0.55
Enhanced ADO-OFDM (without coding)	32	33	0.998
Hamming coding (3,1)	27	28	0.331
Hamming coding (7,4)	28.5	30	0.57
Hamming coding (15,11)	29	30.2	0.732

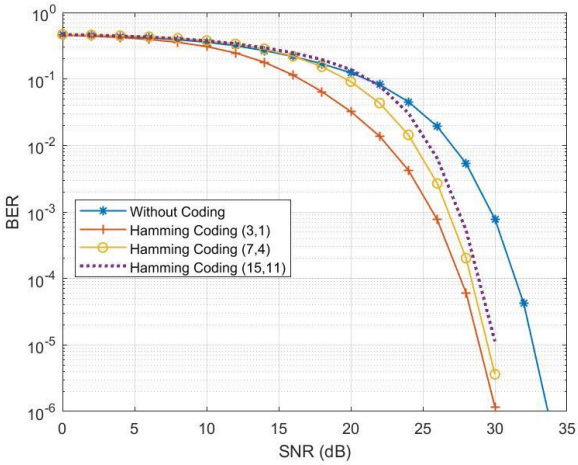

(a)

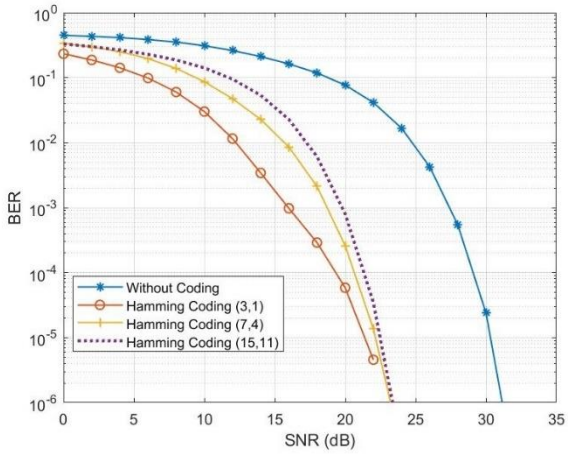

(b)

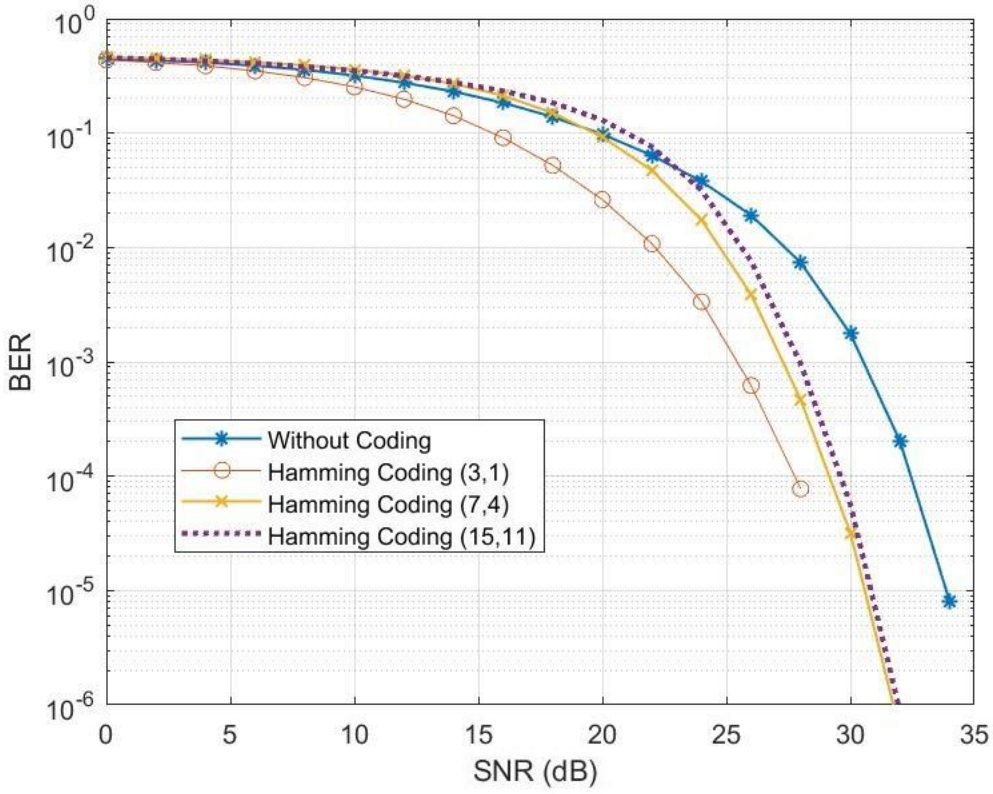

(c)

Fig. 10 BER Performance with Hamming Codes (a) 16QAM DCO-OFDM (b) 256QAM ACO-OFDM (c) ADO-OFDM (16QAM DCO-OFDM,16QAM ACO-OFDM).

Finally, the coverage of VLC inside indoor OWC simulated concerning LOS channel and the simulation parameters as in Table 3. We consider physical room space dimensions (6m, 5m, 3m); four LED sources are distributed in different room ceiling locations. We simulate each transmitter source with a grid (30 x 30) of LEDs to optimize illumination and receiving power. The optical distribution range differs as the values of $\Phi_{½}$ variations. The received power range in dBm for $\Phi_{½} = 70°$ and $30°$ is $-9.5 \leq P_r \leq -3.8$ and $-11 \leq P_r \leq 0.4$ respectively, as shown in Fig 11.

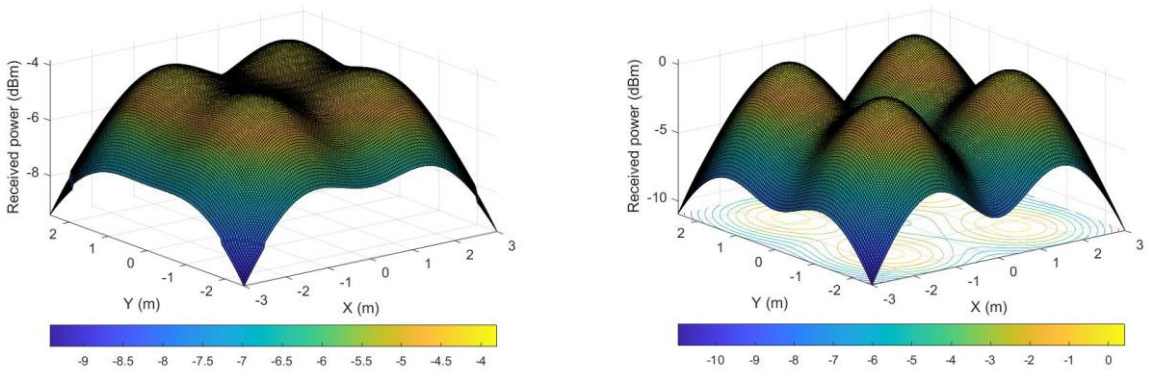

(a) **(b)**

Fig. 11 Optical Power Distribution for $\Phi_{½}$ (a) 70° (b) 30°

Table 3 System Parameter for VLC-OWC

Parameter	Value
LED locations in the ceiling of the room	(1.5,1.25,3);(1.5,3.75,3);(4.5,1.25,3);(4.5,3.75,3)
Transmit Power	20 mw
Total power per grid (30x30)	30x30x20mw = 18w
Half illumination angle	70°; 30°
The physical area of the photodetector	1 cm^2
FOV	60°
Distance between a transmitter to receiver	2m
Lens refractive index	1.5

5-Conclusions

In this paper, we have simulated and tested the LOS channel of OWC based VLC. Various effecting parameters can characterize the optical distribution in an indoor environment, such as transmit power, room dimensions, half illumination angle, FOV angle, and physical area of the photodetector. We have performed IM/DD based on different optical OFDM b to study the performance of OWC/VLC in LOS channels. We proposed an ADO-OFDM system model that reduces the complexity of traditional ADO-OFDM and enhances the VLC performance. The Proposed system gives the best spectral efficiency than ACO-OFDM and the same as DCO-OFDM if it uses the same number of subcarriers. When we use higher constellation modulation with an odd subcarrier, the ADO-OFDM spectral efficiency exceeds the DCO-OFDM. The proposed ADO-OFDM has better optical power efficiency than DCO-OFDM, and ACO-OFDM is the best because it does not use a DC bias. The BER performances are evaluated for OFDM systems; the BER increases if the M order constellation modulation of QAM increases. Different lengths of Hamming channel coding are tested with the optical OFDM systems, and the BER decreases and marking (7,4) as an excellent choice to use in VLC system-based OFDM. As future work, The proposed model can be tested with the diffuse channel, and a hardware model can be implemented using Field Programmable Gate Array (FPGA).

References

[1] M. Z. Chowdhury, M. T. Hossan, A. Islam, and Y. M. Jang, "A Comparative Survey of Optical Wireless Technologies: Architectures and Applications," *IEEE Access*, vol. 6, pp. 9819–9840, 2018, doi: 10.1109/ACCESS.2018.2792419.

[2] N. J. Jihad and S. M. Abdul Satar, "Performance study of ACO-OFDM and DCO OFDM in optical camera communication system," in *2020 2nd Al-Noor International Conference for Science and Technology (NICST)*, Aug. 2020, pp. 63–67, doi: 10.1109/NICST50904.2020.9280319.

[3] E. Calvanese Strinati *et al.*, "6G: The Next Frontier: From Holographic Messaging to Artificial Intelligence Using Subterahertz and Visible Light Communication," *IEEE Veh. Technol. Mag.*, vol. 14, no. 3, pp. 42–58, 2019, doi: 10.1109/MVT.2019.2921162.

[4] M. Z. Chowdhury, M. Shahjalal, M. K. Hasan, and Y. M. Jang, "The role of optical wireless communication technologies in 5G/6G and IoT solutions: Prospects, directions, and challenges," *Appl. Sci.*, vol. 9, no. 20, 2019, doi: 10.3390/app9204367.

[5] M. Saadi, T. Ahmad, M. Kamran Saleem, and L. Wuttisittikulkij, "Visible light communication – An architectural perspective on the applications and data rate improvement strategies," *Trans. Emerg. Telecommun. Technol.*, vol. 30, no. 2, pp. 1–21, 2019, doi: 10.1002/ett.3436.

[6] X. Huang, F. Yang, X. Liu, H. Zhang, J. Ye, and J. Song, "Subcarrier and power allocations for dimmable enhanced ADO-OFDM with iterative interference cancellation," *IEEE Access*, vol. 7, pp. 28422–28435, 2019, doi: 10.1109/ACCESS.2019.2901939.

[7] A. Kumar and S. K. Ghorai, "Effect of multipath reflection on BER performance of indoor MIMO-VLC system," *Opt. Quantum Electron.*, vol. 50, no. 11, 2018, doi: 10.1007/s11082-018-1656-0.

[8] A. Sobhy, S. ElSayed, and A. Zekry, "Enhancing the performance of optical VLC system based on asymmetric symmetric subcarriers OFDM," *Int. J. Commun. Syst.*, vol. 33, no. 10, pp. 1–19, 2020, doi: 10.1002/dac.4226.

[9] N. Sharan and S. K. Ghorai, "PAPR reduction and nonlinearity alleviation using hybrid of precoding and companding in a visible light communication (VLC) system," *Opt. Quantum Electron.*, vol. 52, no. 6, 2020, doi: 10.1007/s11082-020-02426-1.

[10] Z. Wang, T. Mao, and Q. Wang, "Optical OFDM for visible light communications," *2017 13th Int. Wirel. Commun. Mob. Comput. Conf. IWCMC 2017*, no. 1, pp. 1190–1194, 2017, doi: 10.1109/IWCMC.2017.7986454.

[11] J. Armstrong, "OFDM for Optical Communications(Invited Tutorial)," *J. Light. Technol.*, vol. 27, no. 3, pp. 189–204, 2009.

[12] X. Zhang, Y. F. Zhou, Y. P. Yu, P. C. Han, and X. R. Wang, "Comparison and Analysis of DCO-OFDM, ACO-OFDM and ADO-OFDM in IM/DD Systems," *Appl. Mech. Mater.*, vol. 701–702, pp. 1059–1062, 2014, doi: 10.4028/www.scientific.net/amm.701-702.1059.

[13] A. A. Abdulkafi, M. Y. Alias, and Y. S. Hussein, "Performance analysis of DCO-OFDM in

VLC system," *2015 IEEE 12th Malaysia Int. Conf. Commun. MICC 2015*, vol. 1, no. Micc, pp. 163–168, 2016, doi: 10.1109/MICC.2015.7725427.

[14] S. D. Dissanayake, S. Member, J. Armstrong, and S. Member, "Comparison of ACO-OFDM , DCO-OFDM and ADO-OFDM in IM / DD Systems," vol. 31, no. 7, pp. 1063–1072, 2013.

[15] S. E. D. N. Mohamed, A. E. N. A. Mohamed, F. E. A. El-Samie, and A. N. Z. Rashed, "Performance enhancement of IM/DD optical wireless systems," *Photonic Netw. Commun.*, vol. 36, no. 1, pp. 114–127, 2018, doi: 10.1007/s11107-018-0761-0.

[16] R. Mesleh, H. Elgala, and H. Haas, "On the performance of different OFDM based optical wireless communication systems," *J. Opt. Commun. Netw.*, vol. 3, no. 8, pp. 620–628, 2011, doi: 10.1364/JOCN.3.000620.

[17] H. Chen *et al.*, "Performance comparison of visible light communication systems based on ACO-OFDM, DCO-OFDM and ADO-OFDM," *ICOCN 2017 - 16th Int. Conf. Opt. Commun. Networks*, vol. 2017-Janua, pp. 1–3, 2017, doi: 10.1109/ICOCN.2017.8121584.

[18] R. S. J. Godwin, K. Veena, and D. S. Kumar, "Performance analysis of direct detection Flip-OFDM for VLC system," *1st Int. Conf. Emerg. Trends Eng. Technol. Sci. ICETETS 2016 - Proc.*, no. 3, 2016, doi: 10.1109/ICETETS.2016.7603059.

[19] P. P. Jativa, C. A. Azurdia-Meza, M. R. Canizares, D. Zabala-Blanco, and S. Montejo-Sanchez, "Performance Analysis of OFDM-Based VLC Schemes in NLOS Channels," *2020 South Am. Colloq. Visible Light Commun. SACVC 2020 - Proc.*, 2020, doi: 10.1109/SACVLC50805.2020.9129862.

[20] A. N. Kareem, S. M. Abdul Satar, M. A. Husein, L. A. Al-Hashime, and G. A. Al-Suhail, "Performance Improvement Of OOFDM Systems Based On Advanced Logarithmic Companding Technique," *Trans. Networks Commun.*, vol. 6, no. 5, pp. 2–11, 2018, doi: 10.14738/tnc.65.5065.

[21] M. M. Céspedes, B. G. Guzmán, and V. P. Gil Jiménez, "Lights and shadows: A comprehensive survey on cooperative and precoding schemes to overcome LOS blockage and interference in indoor VLC," *Sensors (Switzerland)*, vol. 21, no. 3, pp. 1–41, 2021, doi: 10.3390/s21030861.

[22] O. W. Communications, *Ghassemlooy, Z._ Popoola, W._ Rajbhandari, S - Optical Wireless Communications_ System and Channel Modelling with MATLAB®-CRC Press LLC (2019)*.

[23] X. Zhang, Q. Wang, R. Zhang, S. Chen, and L. Hanzo, "Performance Analysis of Layered ACO-OFDM," *IEEE Access*, vol. 5, pp. 18366–18381, 2017, doi: 10.1109/ACCESS.2017.2748057.

[24] X. Huang, F. Yang, C. Pan, and J. Song, "Advanced ADO-OFDM with Adaptive Subcarrier Assignment and Optimized Power Allocation," *IEEE Wirel. Commun. Lett.*, vol. 8, no. 4, pp. 1167–1170, 2019, doi: 10.1109/LWC.2019.2910250.

[25] R. Mesleh, H. Elgala, and H. Haas, "LED nonlinearity mitigation techniques in optical wireless OFDM communication systems," *J. Opt. Commun. Netw.*, vol. 4, no. 11, pp. 865–875, 2012, doi: 10.1364/JOCN.4.000865.

[26] P. Kumar, A. K. Ahuja, and R. Chakka, "BCH/hamming/cyclic coding techniques: Comparison of PAPR-reduction performance in OFDM systems," *Adv. Intell. Syst. Comput.*, vol. 632, pp. 557–566, 2018, doi: 10.1007/978-981-10-5520-1_50.

[27] M. A. Fleah and Q. F. Al-Doori, "Design and Implementation of Turbo encoder/decoder using FPGA," *1st Int. Sci. Conf. Comput. Appl. Sci. CAS 2019*, pp. 46–51, 2019, doi: 10.1109/CAS47993.2019.9075589.

[28] M. M. A. Mohammed, C. He, and J. Armstrong, "Performance Analysis of ACO-OFDM and DCO-OFDM Using Bit and Power Loading in Frequency Selective Optical Wireless Channels," *IEEE Veh. Technol. Conf.*, vol. 2017-June, pp. 0–4, 2017, doi: 10.1109/VTCSpring.2017.8108403.

Figures

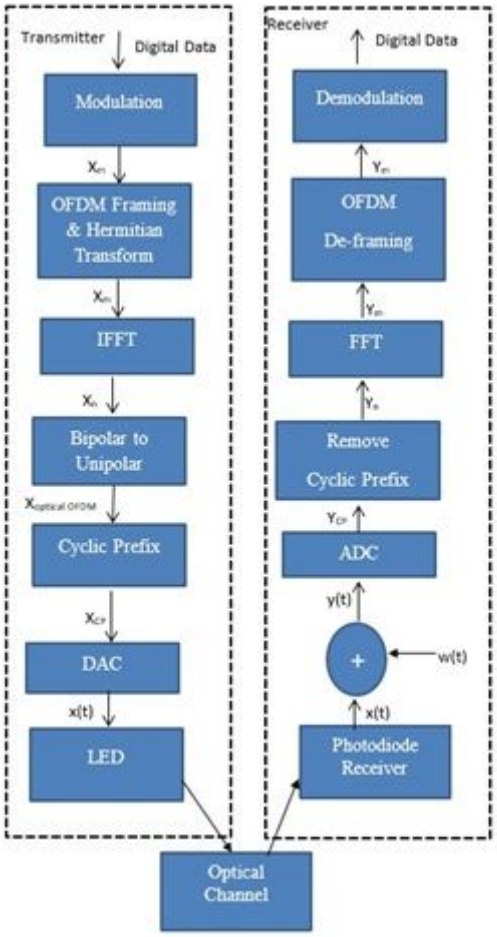

Figure 1

General Optical OFDM System

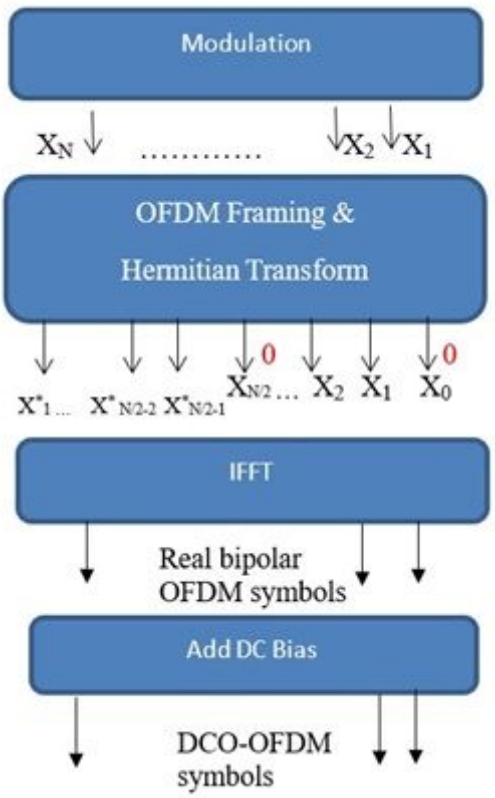

Figure 2

DCO-OFDM Generation System

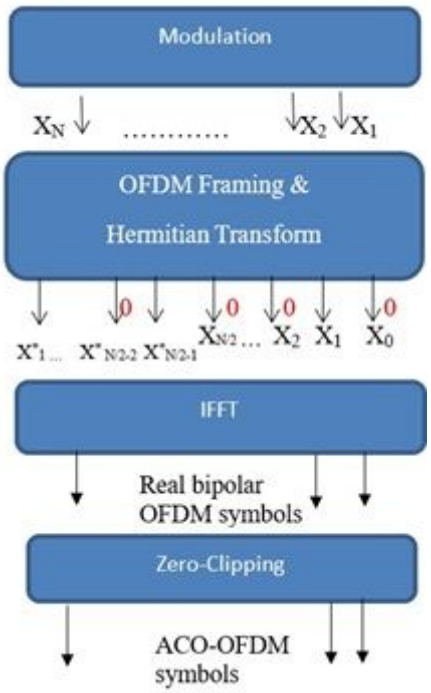

Figure 3

ACO-OFDM Generation System

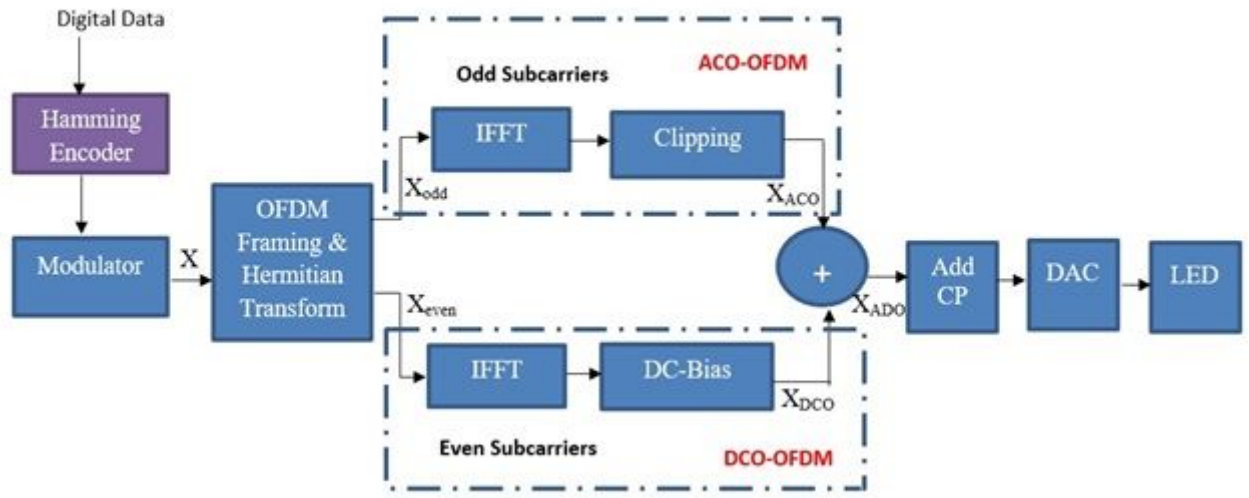

Figure 4

The Proposed ADO-OFDM Transmitter System

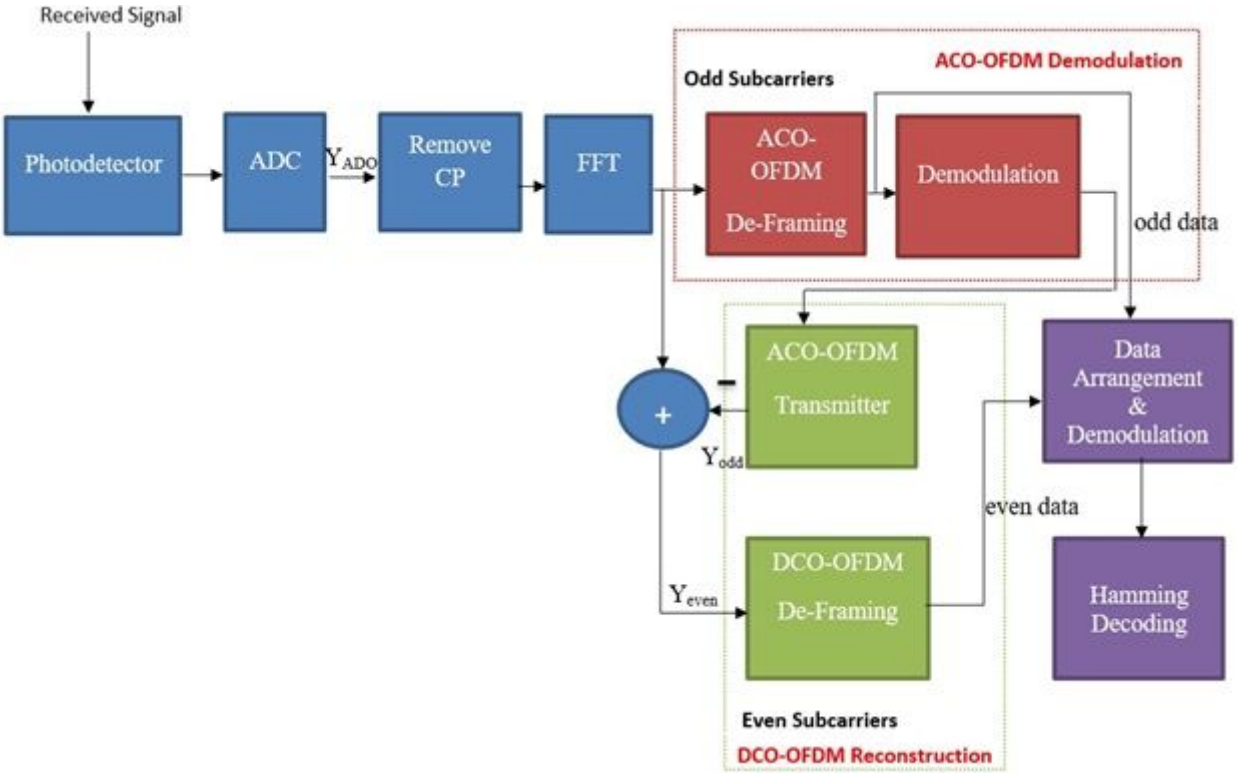

Figure 5

The Enhanced ADO-OFDM Receiver System

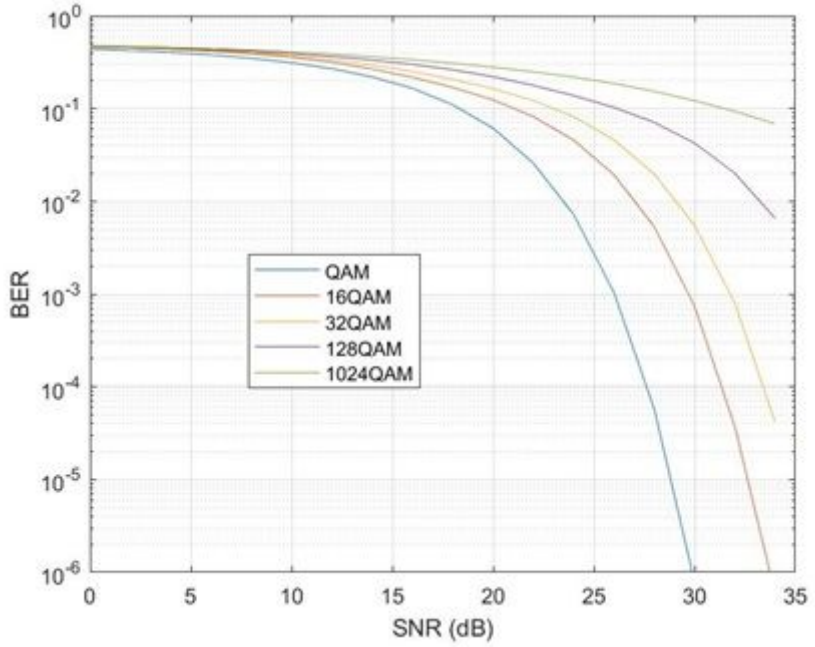

Figure 6

DCO-OFDM BER Performance.

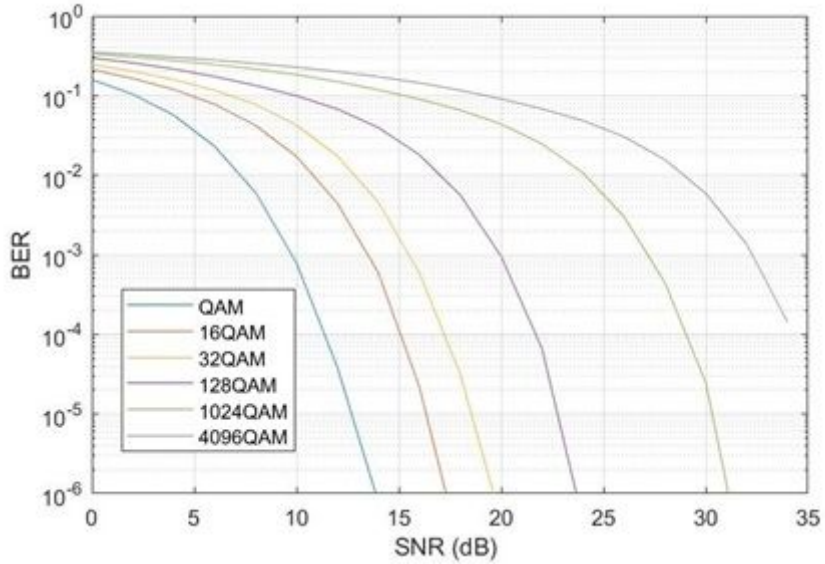

Figure 7

ACO-OFDM BER Performance.

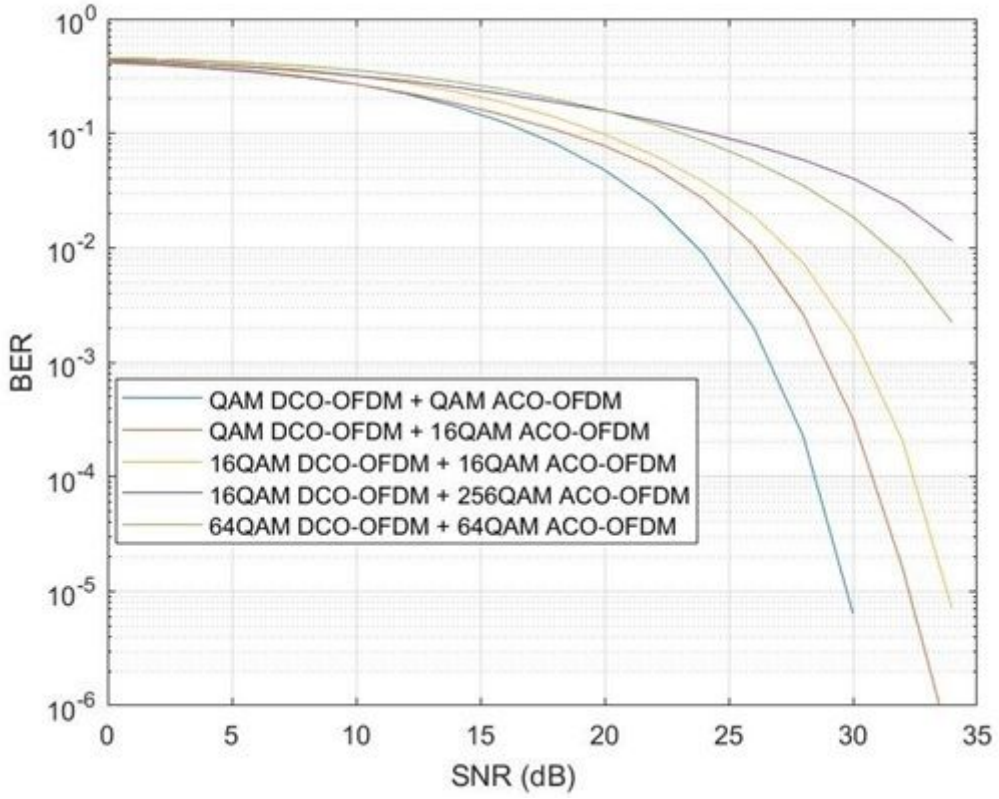

Figure 8

Proposed Enhanced ADO-OFDM BER Performance.

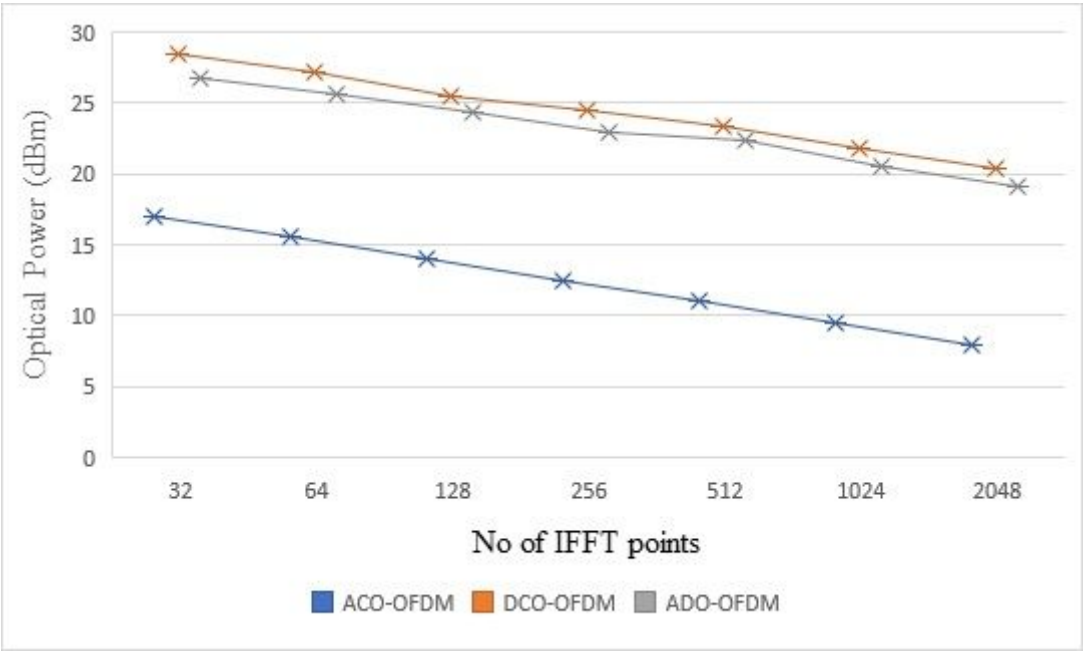

Figure 9

Optical Transmitted Power for Various Optical OFDM Systems.

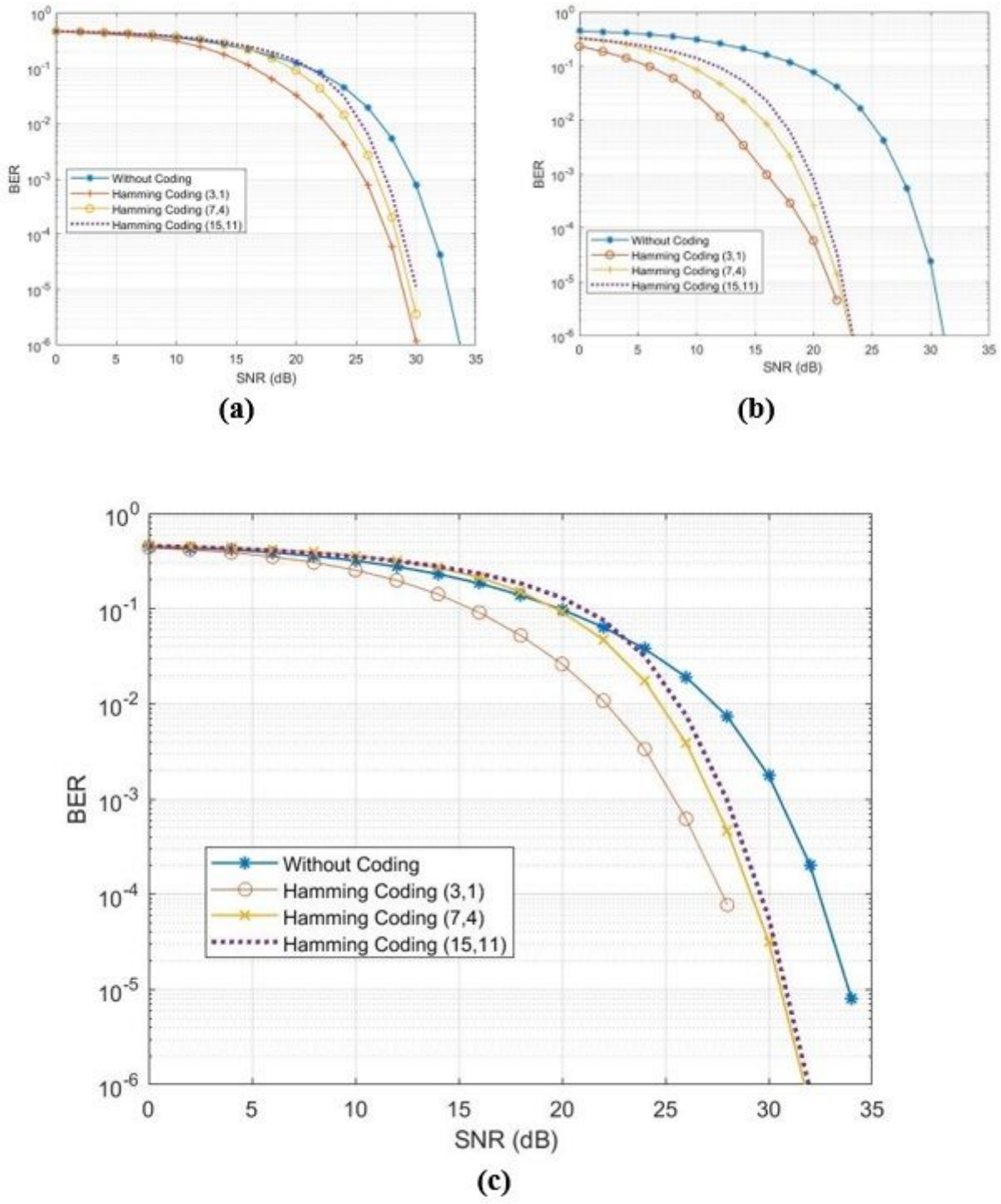

Figure 10

BER Performance with Hamming Codes (a) 16QAM DCO-OFDM (b) 256QAM ACO-OFDM (c) ADO-OFDM (16QAM DCO-OFDM,16QAM ACO-OFDM).

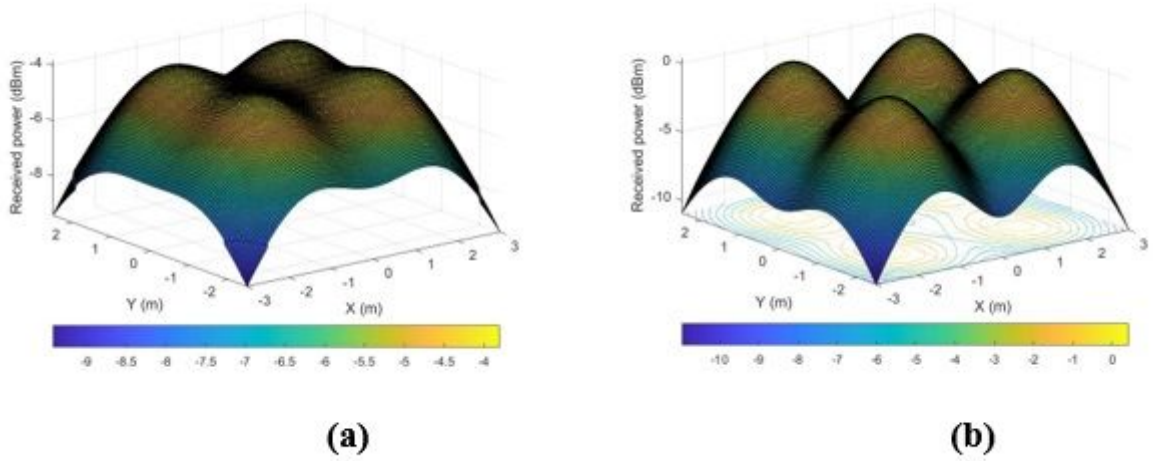

Figure 11

Optical Power Distribution for F½ (a) 70° (b) 30°